

Creation of synergistic effect among raw materials in biodegradable films with novel, designed ZnO particles

Yeliz Köse & Ender Suvacı

To cite this article: Yeliz Köse & Ender Suvacı (2024) Creation of synergistic effect among raw materials in biodegradable films with novel, designed ZnO particles, Polymer-Plastics Technology and Materials, 63:3, 189-202, DOI: [10.1080/25740881.2023.2280621](https://doi.org/10.1080/25740881.2023.2280621)

To link to this article: <https://doi.org/10.1080/25740881.2023.2280621>



Published online: 14 Nov 2023.



Submit your article to this journal [↗](#)



Article views: 205



View related articles [↗](#)



View Crossmark data [↗](#)



Creation of synergistic effect among raw materials in biodegradable films with novel, designed ZnO particles

Yeliz Köse^{a,b} and Ender Suvacı^{a,c}

^aDepartment of Materials Science and Engineering, Eskisehir Technical University, Eskisehir, Turkey; ^bFaculty of Engineering, Department of Metallurgy and Materials Engineering, Bilecik Seyh Edebali University, Bilecik, Turkey; ^cEntekno Corp. R&D Laboratories, Eskisehir, Turkey

ABSTRACT

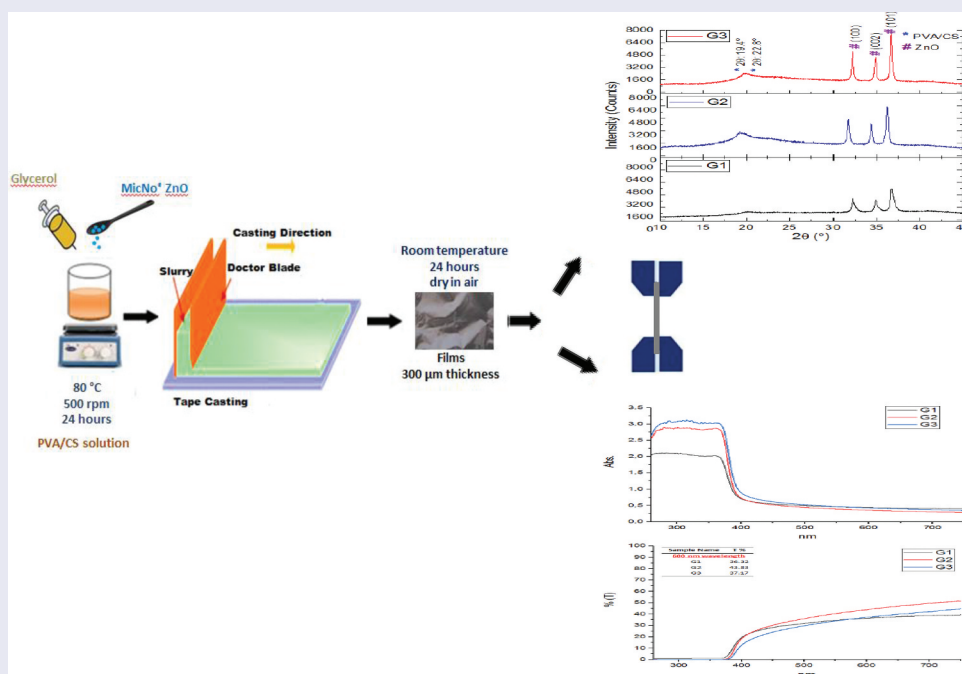
The use of biodegradable polymers in packaging and wound dressing holds great potential for sustainability and a green economy. However, many applications also require high mechanical, thermal and UV-barrier properties. Although nano-metal oxide powders with different morphologies have been tested to meet expectations, the problem of toxicity and uncontrolled agglomeration could not be eliminated. A systematic study of the type of raw materials used and the effects of the amount used remained incomplete. Therefore, the research objective of this study is to interpret the effects of the type of raw materials and the amount of use on the mechanism of synergistic action in achieving the desired properties. The results show the importance of the amount of PVA-glycerol and the molar weight of chitosan for MicNo[®]-ZnO powder doped biodegradable films with new morphology; that includes the advantages of both micron and nano size, to have more effective UV-barrier, mechanical and thermal properties.

ARTICLE HISTORY

Received 2 August 2023
Revised 27 October 2023
Accepted 3 November 2023

KEYWORDS

Chitosan; glycerol; Polyvinyl alcohol; thermal stability; UV-blocking; Zinc oxide



1. Introduction

The use of approximately 15–30 million tons of non-biodegradable polymers every year in the United States and Western Europe^[1] and the fact that we consume oil 100,000 times faster than nature can produce it have led people to the principle of green production.^[2] Using

composite materials based on biodegradable polymers, offering satisfactory waste management, having low toxicity, and reducing greenhouse gas emissions has become mandatory.^[2] The use of these polymers increased by 10% in North America – Europe and 13% in Asia in the 5 years (2009–2014). While the market

capacity of these polymers was 96.4 Billion USD in 2022, it is predicted to reach 215.6 Billion USD by 2030 and grow with a Compound Growth Rate (CAGR) of 10.6% during the 2022–2030 analysis period.^[3] According to the principles of green production in the context of sustainability, products should be efficient during their lifetime but easily degradable at the end of their useful life without requiring a separate effort.^[4] This principle argues for the use of agro-polymers instead of petrochemical-based polymers. However, the low decomposition temperature, weak mechanical strength, and low UV resistance properties of agro-polymers cause problems in their potential use. To solve these problems, blending with natural-synthetic polymers and/or modification with inorganic additives and natural-synthetic fibers is carried out.^[2,5]

Chitosan (CS), one of the agro-polymer types, is a natural polysaccharide obtained from the partial or complete deacetylation of chitin.^[6] Chitosan is used in various forms such as nanoparticles, hydrogels, microcapsules, and films in numerous applications such as agriculture, packaging, biochemistry, pharmaceuticals, wastewater treatment, textile and paper manufacturing, and cosmetics industries because it is biodegradable, biocompatible, nontoxic, and easily moldable. The chitosan source, degree of deacetylation (DDA), molecular weight (MW) and polydispersity index (PDI) are effective to obtain the desired shapes and properties.^[7–9] The degree of deacetylation has a greater effect on the physicochemical properties of the chitosan-based material, such as crystallinity, % absorption, mechanical strength, thermal stability, and degradation rate.^[10,11] In addition to the physicochemical properties, the molecular weight has a greater effect on the biological properties such as antioxidant activity, antibacterial ability, antifungal activity, and wound healing activity.^[12] A synergistic effect between the degree of deacetylation and molar weight cannot be ignored, but the mechanism of action could not be clearly determined in previous studies. Hsu et al.^[13] reported that tensile strength increased when the degree of deacetylation (83–87%) was kept constant and the molecular weight was increased from 204 kDa to 335 kDa. However, they could not explain why the tensile strength increased at a lower degree of deacetylation. In another study by Kofuji et al.,^[14] the researchers kept the degree of deacetylation of chitosan constant (86–87%) and increased the molecular weight of chitosan; they observed that the rate of degradation decreased in lysozyme solution. While there are extensive studies on the effect of the molar weight of chitosan on biological properties, studies on its effect on physicochemical properties are limited. Chitosan's low solubility in neutral or high pH organic solvents, low mechanical

strength, and reduced antibacterial activity at pH > 6.5 due to inter- and intramolecular hydrogen bonding limit its potential applications. Therefore, blending processes with synthetic or natural polymers are applied to improve the physicochemical properties, facilitate the fabrication, and increase the biocompatibility and biological activity.^[15,16]

In recent studies in the field of biomedicine and biomaterials, the use of PVA agro-polymers in improving their properties or using them with additives instead of petroleum-based polymers has increased due to their biocompatibility, low cytotoxicity, degradability, advanced mechanical and thermal properties.^[2,17] PVA is a synthetic biodegradable polymer with chitosan to create high tensile strength and flexible biodegradable films by providing high film-forming ability and homogeneous distribution of added inorganic substances.^[18–22] In the study by Kim et al.,^[23] it was demonstrated that with increasing PVA concentration, the intramolecular/intermolecular hydrogen bonding between the hydroxyl groups of PVA and the Zn⁺² ions increased. As a result, a homogeneous distribution of the inorganic powders on the film surface was achieved, an increase in strength, a decrease in the percentage water absorption capacity, and an increase in UV barrier properties were observed. In the study conducted by Huie et al.,^[24] it was observed that the cost-performance ratio of the films was improved as a result of providing sufficient hydrophobicity, thermal stability, UV protection, and mechanical and barrier properties, thanks to the synergistic role created by the hydrogen bonding of PVA and chitosan.

Although the components chitosan and glycerol are hydrophilic, glycerol is a hygroscopic component with a stronger tendency to attract water molecules than chitosan. In the study of Priyadarshi et al.,^[25] it was observed that the % water absorption capacity of the films decreased when the amount of glycerol was kept constant and the amount of chitosan was increased. As the presence of free hydroxyl and amine groups decreases due to the interaction of glycerol and chitosan, a decrease in the moisture content of the films is observed. A similar tendency was observed in chitosan films containing citric acid and glycerol.^[25] The variation of moisture content can have a significant effect on the functional properties of the films, for example, on the mechanical properties.^[26] The plasticizing effect of glycerol predominates in the mechanical behavior of composite films in samples containing both glycerol and chitosan. As the amount of glycerol increases, a decrease in tensile strength and an increase in elongation at break are observed in the study by Vasquez et al.,^[27]

and a reduction in transmittance values in UV-visible regions is kept in the study by Cazon et al.^[28] Increasing the amount of glycerol increases the diffusion of chitosan in the polymer matrix and provides a uniform and homogeneous surface. Due to its hydrophilic nature, physical water can evaporate at higher temperatures ($\geq 110^\circ\text{C}$), which is due to strong water-glycerol interactions when glycerol content is increased. In the study of Vázquez et al.,^[29] it was found that the increase in chitosan content and the decrease in glycerol content improved the thermal stability properties of the samples and reduced the weight loss.

All these results indicate that the combination of chitosan, PVA and glycerol in the right amounts and in the right form is crucial to obtain the desired properties and should be optimized for each new composition. However, a systematic study on the effects of the type of raw material used and the amount used remains a research gap in the literature.

Inorganic fillers are commonly used in polymer matrices to improve mechanical and thermal properties and UV resistance. Nanoparticles are the most commonly used fillers. Unfortunately, the poor performance and process limitations of biodegradable polymers for certain applications mostly depend on the size, chemical composition, and morphology of the added nanoparticles.^[30] In our previous work,^[31] it was observed that the addition of nanosized ZnO to the polymer matrix did not affect the transparency of the films but reduced the local mechanical strength due to non-uniform distribution in the polymer matrix because of the uncontrolled agglomeration tendency of the nanoparticles, which have a very high surface energy. Therefore, our previous^[29] and current study used MicNo[®]-ZnO particles designed as micrometer-sized hexagonal platelets consisting of primary fine particles. Thus, increases both in UV barrier property and mechanical strength were observed due to the superior surface coverage (up to 70% more) of MicNo[®]-ZnO with respect to ZnO nanoparticles. The results clearly showed that MicNo[®]-ZnO is much more compatible with the polymeric matrices than the nanoparticles. Therefore, new biodegradable polymer-based composites should be preferably prepared by MicNo[®]-form fillers.

Consequently, this study's research objective was to understand the relationships between PVA and glycerol amounts, chitosan molecular weight, and mechanical, thermal, and UV properties in the presence of novel MicNo[®]-ZnO fillers

2. Experimental procedure

2.1. Materials

Three types of chitosan, those from Sigma- Aldrich Co. LLC, with low (molecular weight of 40 kDa), medium (molecular weight of 140 kDa), and high molecular weight (molecular weight of 210 kDa) and a deacetylation degree of 75% were used. In addition, PVA with a degree of hydrolysis of 99% and a molecular weight of 146,000–186,000, glacial acetic acid and glycerol from Sigma-Aldrich Co. LLC were used. Undoped inorganic MicNo[®]-ZnO powders with 2–10 μm hexagonal platelet aggregates of 30–100 nm sized particles were supplied by Entekno Materials Inc.

2.2. Preparation of composite films

In previous studies,^[31] the amount of MicNo[®]-ZnO was varied (between 0.5 g and 2.5 g), and since the best distribution was observed in 1.5 g additives, the MicNo[®]-ZnO additive amount was kept constant at 1.5 g in our study.

2.2.1. By the concentration of PVA

PVA (5–15% v/w) was dissolved at 80°C and stirred at 500 rpm for 24 hours. Then MicNo[®]-ZnO (1.5 g) was added to the PVA solution at 80°C and stirred until it became a gel-like viscous solution. The resulting solution was poured onto a plastic substrate using the tape casting technique to obtain films with a thickness of 300 μm and dried at room temperature for 24 hours.

2.2.2. By chitosan molecular weight

Low, medium, and high molecular weight CS (3% v/w) in 3% aqueous acetic acid solution and PVA (5–15% v/w) in 80°C water were dissolved for 24 hours. After that, the PVA solution (30 mL) was added to the CS solution (20 mL) while it was being magnetically stirred to get a clear solution. MicNo[®]-ZnO (1.5 g) and glycerol (10 mL) were added to the PVA/chitosan solution, and the resulting viscous solution was poured onto the plastic floor to form a 300 μm thick film, and dried at room temperature for 24 hours.

2.2.3. By the amount of glycerol usage

Low molecular weight of CS (3% v/w) in 3% aqueous acetic acid solution and PVA (5–15% v/w) in 80°C water were dissolved for 24 hours. After that, the PVA solution (30 mL) was added to the CS solution (20 mL) while it was being magnetically stirred to get a clear solution. Then, MicNo[®]-ZnO (1.5 g), three different amounts of glycerol (9-13-17 v.%) were added into the PVA/chitosan and the resulting viscous solution was poured onto

Table 1. Composition of the composite films, prepared and tested in this study.

Sample Name	Sample
P1	PVA film contained 5 (wt.%) PVA
P2	PVA film contained 15 (wt.%) PVA
C1	PVA/chitosan film contained high molecular weight of chitosan
C2	PVA/chitosan film contained medium molecular weight of chitosan
C3	PVA/chitosan film contained low molecular weight of chitosan
G1	PVA/chitosan film contained 9 (v.%) glycerol
G2	PVA/chitosan film contained 13 (v.%) glycerol
G3	PVA/chitosan film contained 17 (v.%) glycerol

the plastic floor to form a 300 μm thick film, and dried at room temperature for 24 hours. Table 1 shows the designations of the samples that were prepared and tested in this study. Before the tests, the films were cut into specific sizes, widths, and lengths.

2.3. Materials characterization

The phase analyses of the films were performed by XRD (D2 Phaser Bruker, $\text{Cu K}\alpha = 1.54 \text{ \AA}$). The scanning rate was $2^\circ/\text{min}$, and the 2θ range was between 10° and 45° . The films' upper surface morphologies were examined using scanning electron microscopy (SEM EVO 50 LP, Zeiss, operating at 10 kV). Absorbance and transmittance profiles of the films were recorded by UV-VIS-NIR spectrophotometer (UV-3600 Plus UV-VIS-NIR, Shimadzu) in a wavelength range of 260–750 nm, covering both UV and visible ranges. The mechanical tests were performed by a universal testing machine (INSTRON 5581) according to the ASTM D882 standard method. For these mechanical tests, 5 samples for each film type were cut into 100 mm length and 20 mm width strips. % swelling capacities of the films as a function of pH (i.e., at pH 5–7–9) were determined by the % swelling analysis at 25°C ambient temperature for 2 hours application time. Thermogravimetric-Differential Thermal Analysis (TG-DTA) (TA Q600) evaluated the films' relative thermal stability in the $0\text{--}500^\circ\text{C}$ temperature range, $10^\circ\text{C}/\text{min}$ heating/cooling rate, and nitrogen environment. The biodegradation test was carried out by burying it in the ground at a depth of 10 cm for 14 days.

3. Results and discussion

3.1. Effects of PVA and glycerol amounts, and chitosan molecular weight on structure development of the MicNo[®]-ZnO containing films

The x-ray diffraction patterns of the films are shown in Figure 1. The XRD patterns show that the studied films

correspond to single phase ZnO with close-packed hexagonal wurtzite type crystal structure (JCPDS card no: 36–1451).^[32] Figure 1a shows three characteristic peaks in the XRD patterns of pure PVA films. These are $2\theta = 20.11^\circ$ ($d = 4.412 \text{ \AA}$, (101)), $2\theta = 27.86^\circ$ and $2\theta = 29.21^\circ$ peaks showing the semi-crystalline structure.^[33] Figure 1a shows that as the PVA concentration increased, the intensity of the characteristic peaks of the ZnO and PVA increased. This fact shows that as the PVA concentration increases, the intermolecular interactions of the PVA chains, which increase the crystallization in the composite structure, become more robust, the viscosity of the solution increases, and thanks to the hydrogen bonds formed between Zn^{+2} ions and PVA, the tendency to agglomerate is reduced, causing the homogeneous distribution of inorganic powders.^[19] Therefore, the XRD peak intensity of sample P2 is higher than sample P1. Figure 1b shows three characteristic peak formations in PVA/chitosan films. These are the $2\theta = 11.3^\circ$ peak representing the crystalline phase and the $2\theta = 19.4^\circ$ and $2\theta = 22.8^\circ$ peaks representing the amorphous phase.^[34] While the crystal phase peak was not obtained in the samples we obtained, the amorphous phase peaks were obtained. This indicates that the time elapsed during the casting process after the chitosan has dissolved in acetic acid is shorter than the time required to crystallize the chitosan. Figure 1b shows that characteristic peaks of ZnO could not be obtained in high molecular weight chitosan films (C1). This proves that a high concentration of acetic acid causes degradation of the original structure of ZnO inorganic powders in the PVA/chitosan matrix. It is seen that the characteristic peak intensities of ZnO of the films prepared with medium molecular weight chitosan (C2) are higher than the films prepared with low molecular weight chitosan (C3). This is because as the molecular weight increases, the entanglement factor of the polymer chains and the intermolecular interactions increase, resulting in a homogeneous distribution of ZnO throughout the film.^[35] Figure 1c shows that the intensity of characteristic peaks of ZnO increases with increasing glycerol content. This is due to the presence of –OH groups in the glycerol molecule, which increases the conversion of Zn^{+2} to ZnO. The –OH groups act as templates for the formation of uniformly dispersed ZnO nanoparticles.^[36] Besides, glycerol, which was found to decrease the compatibility, could result in a higher crystallinity for the blend since both phases are less interacted with each other and, thus, can more freely participate in the crystallization process.^[20]

Figure 2 shows SEM micrographs of the films studied in this work. Figure 2a shows that as the

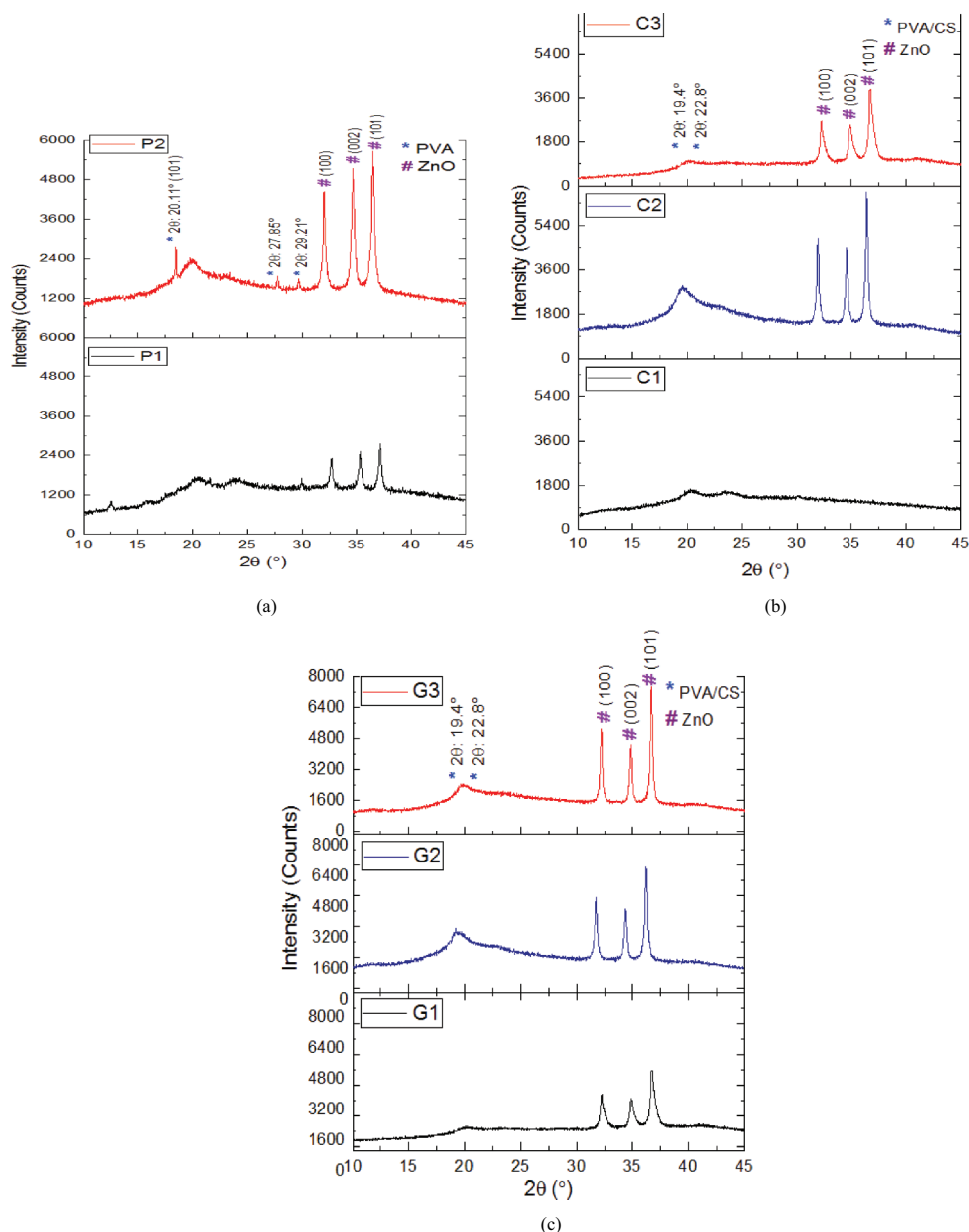


Figure 1. XRD patterns of the films with (a) P1&P2 (b) C1-C3 and (c) G1-G3 compositions.

PVA concentration increased, the inorganic powders were homogeneously dispersed in the film and showed no agglomeration tendency. Probably, due to the hydrogen bonds formed between the components of the mixture, a smooth surface and less agglomeration tendency are observed.^[37] This finding was also demonstrated by XRD and UV-Vis analysis. Figure 2b shows that in high molecular weight chitosan used films, ZnO inorganic powders were not observed in the film matrix because of the dissolution process in high concentration acetic acid solution. The tendency to agglomerate was less in films using low molecular weight chitosan. It showed

a smooth, continuous, and homogeneously dispersed film form without phase separation. The results showed that mol. wt. had no significant effect on the morphology of chitosan films. Figure 2c shows that as the amount of glycerol increased, the agglomeration tendencies of ZnO inorganic powders decreased on the film surface. The slightest tendency to agglomerate was observed in films with 17 (v.%) glycerol. These results are also supported by XRD analysis. The high hydroxyl group content of PVA and glycerol provides a homogeneous distribution in the matrix, forming the basis for converting Zn + 2 to ZnO.^[38]

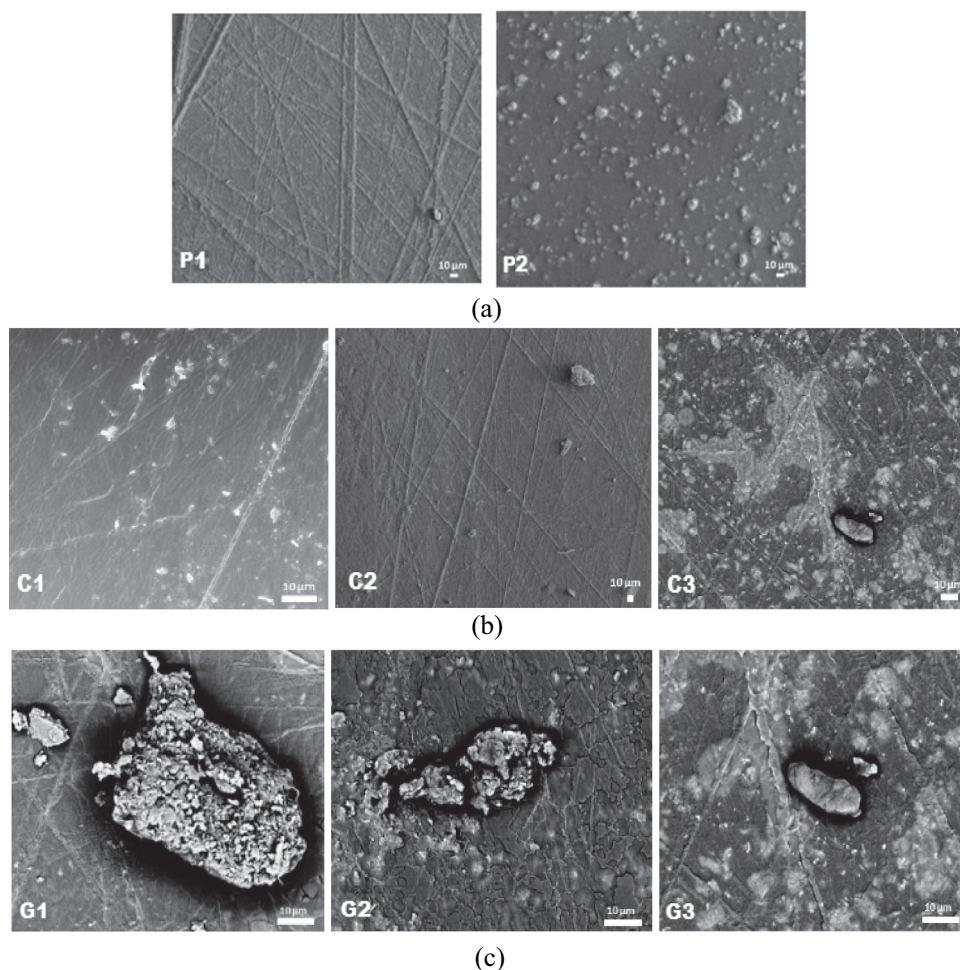


Figure 2. SEM micrographs of the films with (a) P1&P2 (b) C1-C3 and (c) G1-G3 compositions.

3.2. Effects of PVA and glycerol amounts, and chitosan molecular weight on properties of the MicNo[®]-ZnO containing films

3.2.1. Optical properties

Figure 3 shows the UV-Vis absorbance spectra of the films evaluated in this study. The components of the films play a key role in describing their transparency and color parameters.^[39] In Figure 3a, as the PVA concentration increases, the absorbance values in the UV region increase, while the % transmittance value at 600 nm wavelength (the visible range (400–700 nm)) decreases. Because pure PVA has a strong ability to absorb radiation between 200–400 nm.^[40] In addition, as the PVA concentration increases, the formation of intramolecular/intermolecular hydrogen bonds between the hydroxyl groups of PVA and the Zn⁺² ions increases and inorganic powders are homogeneously dispersed.^[23] In Figure 3b, as the molecular weight of chitosan decreases, the absorbance values in the UV region increase, while the % transmittance value at

600 nm wavelength (the visible range (400–700 nm)) decreases. The relationship between the molecular weight of chitosan and the transparency of the films has not been studied in the literature. Absorbance property in the UV region is associated with two distant UV-chromophoric monomers, namely N-acetylglucosamine and glucosamine.^[41] In Figure 3c, as the amount of glycerol increases, the absorbance values in the UV region increase, while the % transmittance value at 600 nm wavelength (the visible range (400–700 nm)) decreases. Because as the amount of glycerol increases, the hydroxyl groups in the glycerol act as templates for the formation of uniformly dispersed ZnO nanoparticles.^[36] Our findings were consistent with the results of the study by Cazón et al.^[28]

3.2.2. Mechanical properties

Table 2 shows the average tensile strength (MPa) and % elongation values of the films evaluated in this study. PVA concentration increases average tensile strength

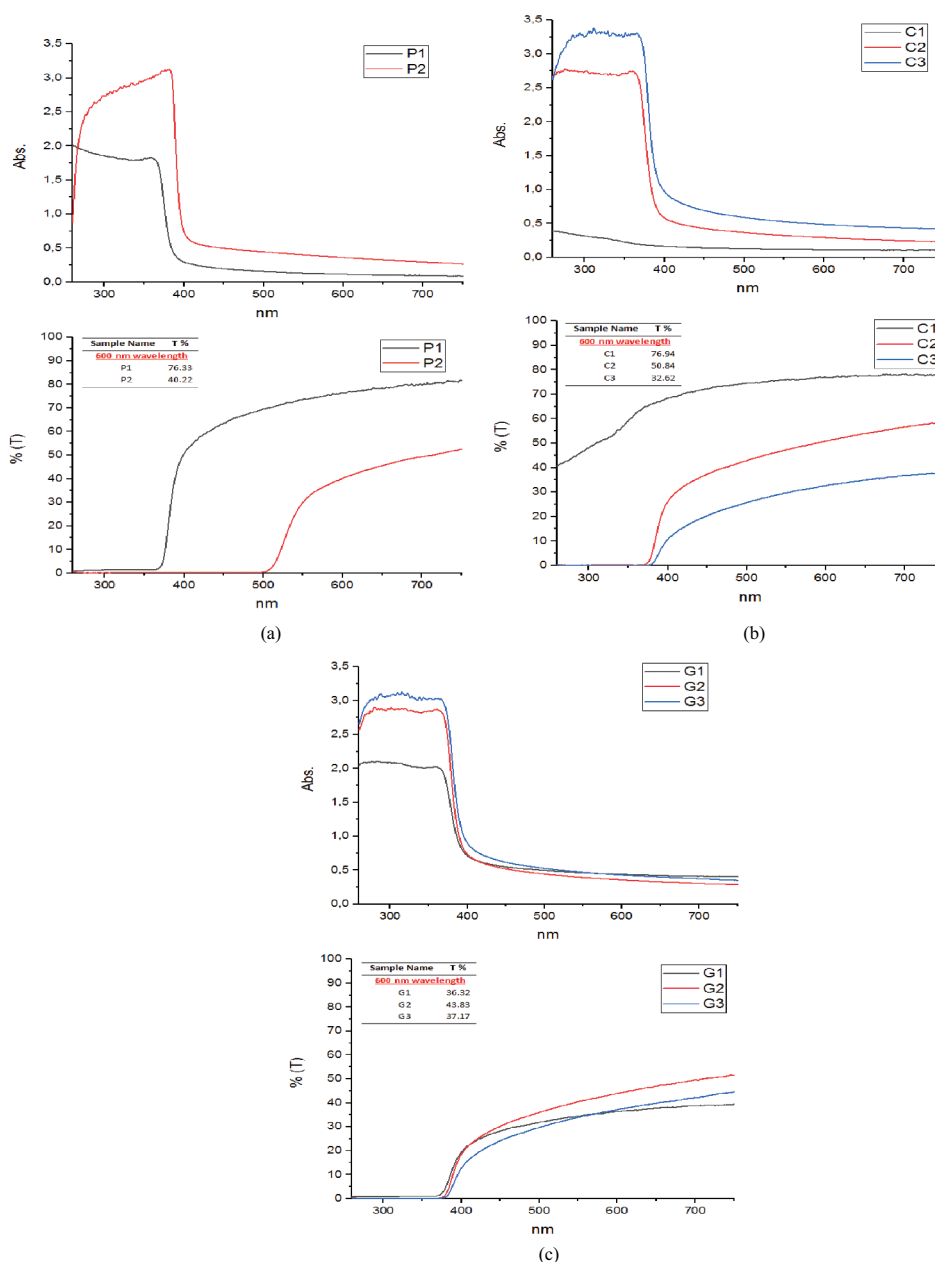


Figure 3. UV-vis absorbance and UV-vis transmittance spectra of the films with (a) P1&P2 (b) C1-C3 and (c) G1-G3 compositions. (the transmittance values of the studied films at 600 nm wavelength given as inlet).

Table 2. Average tensile strength (MPa) and % elongation values of the films.

Sample Name	Average Tensile Strength (MPa)	Average Elongation (%)
P1	.25	6.27
P2	.44	10.46
C1	1.88	75.25
C2	1.44	64.01
C3	1.21	25.52
G1	1.19	26.03
G2	1.12	44.44
G3	1.02	51.41

and considerably enhances the films' % elongation capacity and flexibility. These results supported the positive effects of hydrogen bonds between PVA and Zn^{+2} ions.^[21] PVA addition could improve the mechanical properties of chitosan film, which was in agreement with other reports.^[42,43] The mechanical properties of PVA/chitosan films indicated that PVA polymer greatly influenced the tensile stress and % elongation, while the intermolecular hydrogen bonds formed between amine and hydroxyl groups of two polymers.^[22,44] Variations

in tensile stress values in chitosan films could be due to several factors, including chitosan's molecular weight, source, film preparation, and storage.^[45] As the molecular weight of chitosan increases, tensile strength, and % elongation increase, the high molecular weight of chitosan in the films increased the stiffness of the prepared materials due to its stiffer polymer chain and the existence of inter- and intra-molecular hydrogen bonds.^[46] The relationship between the molecular weight of chitosan and the % elongation of the films has yet to be studied in the literature. As the glycerol content increases, % elongation increases while the tensile strength decreases. Glycerol, which contains many hydroxyl groups in its structure, enters between polymer chains, disrupts intermolecular hydrogen bonds, and causes macromolecules to slip.^[47]

3.2.3. Thermal properties

A polymeric material's thermal stability depends on the macromolecules' nature and interaction ability. When the applied thermal energy exceeds the bond dissociation energy of chemical bonds, it causes chain cleavage or bond dissociation of macromolecules. The thermal decomposition behavior of the films analyzed by TGA/DTG is shown in Figure 4. The thermal parameters, including the maximum temperature of degradation and the total weight loss, are summarized in Table 3. TGA results exhibit three distinct weight loss stages for the studied films in this work.^[48] The first stage of weight loss occurs between 65 and 125°C, which is responsible for removing physisorbed water molecules. The second step, weight loss, which occurs in the temperature range of 150–350°C, overlaps the structural dissociation of hydrogen bonds, deacetylation of chitosan, and depolymerization of PVA. The most critical decomposition temperature is the peak decomposition temperature at which we obtain the maximum weight loss ratio (T_p). The third stage degradation, which occurs in the temperature range of 350–500°C, corresponds to the dissociation of polyene residues, the hydrogen bond between the NH_2 and the $-\text{OH}$ functional group. The thermal decomposition of all samples is of similar patterns. However, the P1 sample has higher thermal stability than the P2 sample. The onset degradation temperature of the nanocomposites increased from 291 to 292°C with an increase in the concentration of PVA (Figure 4a). The improvement in thermal stability is due to the presence of hydrogen bonds, which reduce the permeability of the material's volatile degradation products by acting as a barrier.^[49] As the molecular weight of chitosan increases, the interaction between amine groups and ZnO increases, and polymer segment mobility decreases.^[50] This causes the

degradation of temperature and thermal stability to increase. We can say that the reason for the decrease in the degradation temperature in the C3 sample is due to the deterioration of the structure of ZnO powders in the matrix as a result of the use of high concentrations of acetic acid (Figure 4b). With the increase of the amount of glycerol (Figure 4c), the increased mobility of the mixture components, which facilitates the formation of hydrogen bonds, leads to the improvement of thermal stability.^[46]

3.2.4. Swelling characteristics

Table 4 shows the % swelling of the studied films in this work. Factors affecting the swelling properties of films are i) crosslinking agent ratio, ii) ambient pH, iii) ambient temperature, and iv) application time. Therefore, analyzes were performed at three different environmental pH (5, 7, 9). In a neutral environment ($\text{pH} = 7$), $-\text{OH}$ and $-\text{NH}_2$ polar groups desire to interact with water molecules to form hydrogen bonds. The neutral environment does not change the polarities of polar groups and, therefore, their interactions with water molecules. As a result, the swelling tendency of the polymer is at its maximum value in a neutral environment ($\text{pH} = 7$) according to different pH values.^[51] In an acidic environment ($\text{pH} = 5$), the polar groups of PVA and chitosan chains are protonated, and the positive charge ratio increases, which increases the mutual repulsion with water molecules. As a result, the swelling tendency of the polymer is reduced.^[52] In an alkaline environment ($\text{pH} = 9$), the amine groups are strongly deactivated, and the lone electron pairs on the nitrogen atoms become unusable due to mutual repulsion with the hydroxyl groups in the environment. As a result, the interaction between amine groups and water molecules is blocked, reducing the polymer chains' swelling.^[53] Since the crystal areas in the film structure delay the water diffusion into the film, they prevent the film from swelling and dissolving quickly.^[19] As the PVA concentration increased, a decrease in the % swelling capacity was observed due to the increase of the crystalline regions and the 3-D network structure.^[23] The number of hydrogen bonds and the electrostatic repulsion of neighboring molecules are essential factors in determining the behavior of chitosan, a hydrophilic polyelectrolyte.^[54] Since the films using high and medium molecular weight chitosan have less amorphous structure, the % swelling ratio is lower than those using low molecular weight chitosan.^[19] Adding glycerol to the PVA/chitosan blends caused a further decrease in polar component values, indicating the polyols' participation in intermolecular hydrogen bond formation. With the addition of glycerol, the mobility of

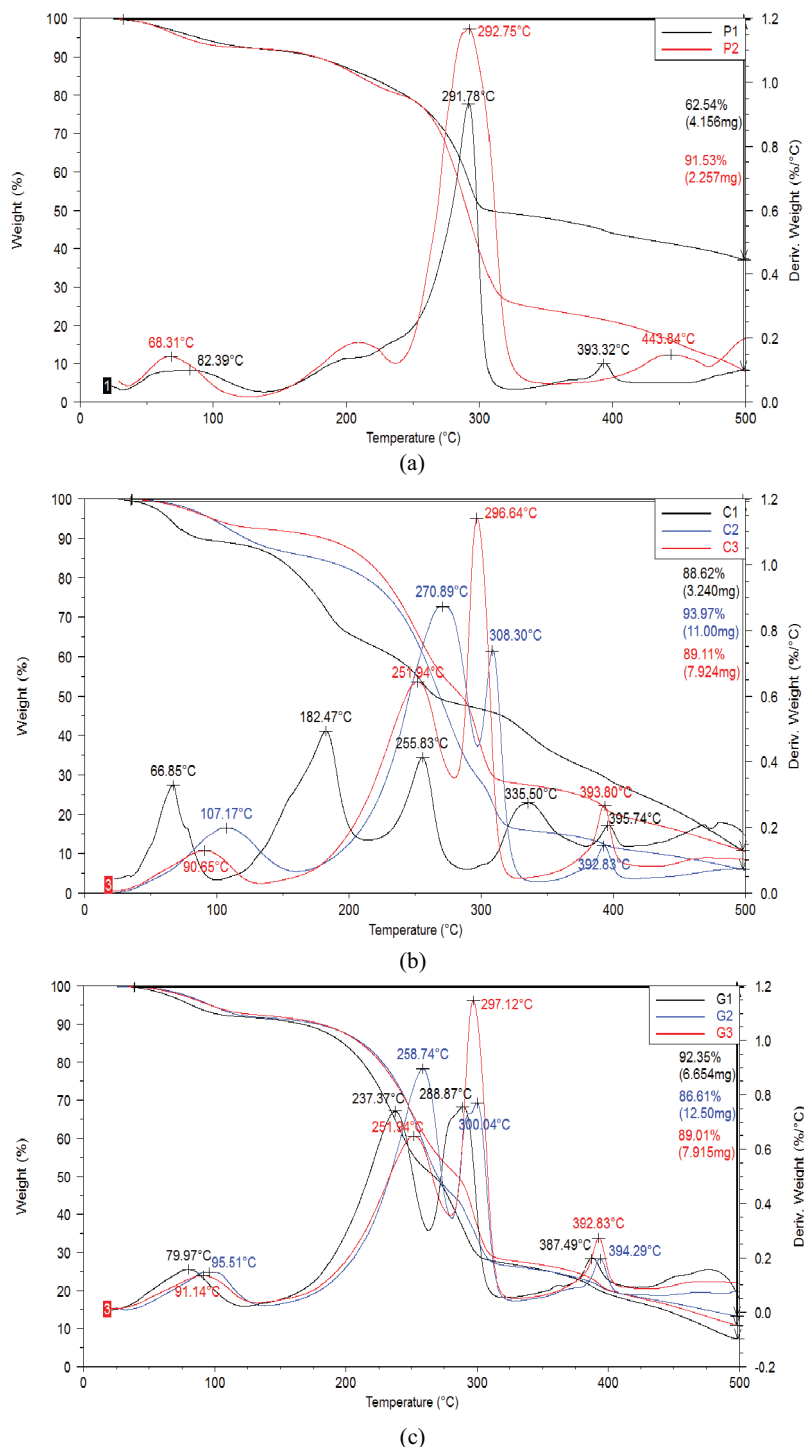


Figure 4. TGA/DTA spectra of the films with (a) P1&P2 (b) C1-C3 and (c) G1-G3 compositions.

the components that trigger the formation of hydrogen bonds increased.^[46] Therefore, as the glycerol content increased, a decrease in the % swelling capacity was observed. The % swelling capacity of films increased steadily as pH increased, reaching up to maximum at neutral (pH = 7), which decreased further at higher pH of the media.^[55]

3.2.5. Biodegradability in soil

The prepared films (1 g) were buried in the soil to a depth of 10 cm, and the moisture content of the soil was kept at a certain level by sprinkling water regularly. After 14 days, they were removed from the soil, washed with deionized water, and dried at 60°C until the weight of the films did not change. The following formula

Table 3. The thermal parameters of the films.

Sample Name	T _{max} (°C)			Total Mass Loss (%)
	Stage 1	Stage 2 (Tp)	Stage 3	
P1	82.39	291.78	393.32	62.54
P2	68.31	292.75	443.84	91.53
C1	66.85	255.83	395.74	88.62
C2	107.17	308.30	392.83	93.97
C3	90.65	296.64	393.80	89.11
G1	79.97	288.87	387.49	92.35
G2	95.51	300.04	394.29	86.61
G3	96.14	297.12	392.83	89.01

calculated the degradation percentage of biodegradable films:

$$I_s(\%) = \frac{(w - w_i)}{w} \times 100\%$$

where w and w_i are the initial weight and the weight at 14 days of buried time of the films after being washed and dried.^[56]

The rates of biodegradation rate of the films are shown in Table 5. Figure 5 shows biodegradation behavior of the biodegradable films in soil. The dominant factor in the biodegradability test in soil is the swelling of the films according to their % water absorption capacity in connection with their hydrophilic properties and the weakening of the polymer chains due to moisture due to further osmosis of moisture entering the polymer network. Later, under the influence of bacteria in the soil, the film's surface becomes rough, voids are formed, and the structural integrity of the film is disrupted, resulting in weight loss.^[56] These results are also supported by % swelling analysis.

3.3. Performance summary of films containing MicNo®-ZnO by PVA and glycerol amounts and chitosan molecular weight

It is desired that the films have low agglomeration tendency, high absorption in the UV region, low opacity value, low brittleness, high thermal resistance, low % water absorption values at pH = 7 and high % biodegradation rate. The effects of variables on the properties of MicNo®-ZnO doped PVA:chitosan films are summarized in Table 6. Homogeneous distribution of inorganic powders across the film surface in thin films prevents local mechanical strength losses, causes an increase in barrier properties in the UV region, increases the films' thermal resistance, and reduces the % swelling capacity. When we look at the intersection of the features, it was seen that all the features we wanted were found in the films using low molecular weight chitosan with 15 (wt. %) PVA and 17 (v.%) glycerol.

Table 4. The % swelling of the films.

Sample Name	Swelling%		
	pH=5	pH=7	pH=9
P1	53.58	93.99	53.26
P2	15.52	33.11	15.47
C1	22.22	25.25	16.92
C2	27.01	34.18	25.17
C3	30.90	41.00	32.16
G1	26.87	75.45	65.06
G2	20.35	52.37	28.52
G3	13.09	41.00	25.17

Table 5. The % biodegradation rate of the films.

Sample Name	% Biodegradation Rate
P1	92.28
P2	46.53
C1	42.28
C2	48.81
C3	52.34
G1	83.17
G2	70.25
G3	52.34

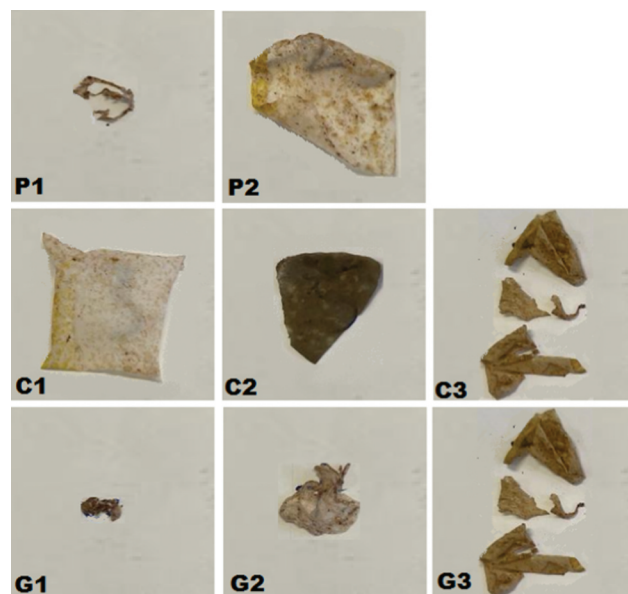
**Figure 5.** Films subjected to degradation by 14 days.

Table 6. Effect of variables on the properties of MicNo[®]-ZnO doped PVA:chitosan films.

Sample Name	Properties							
	Homogeneous distribution	Degree of crystallinity	Absorption UV	Absorption visible	Flexibility	Thermal resistance	% Swelling capacity (pH7)	% Biodegradation Rate
P1	Low	Low	Low	Low	High	Low	High	High
P2	High	High	High	High	Low	High	Low	Low
C1	High	Medium	High	High	High	Medium	Low	Low
C2	Medium	High	Medium	Medium	Medium	High	Medium	Medium
C3	Low	Low	Low	Low	Low	Low	High	High
G1	Low	Low	Low	Low	Low	Low	High	High
G2	Medium	Medium	Medium	Medium	Medium	Medium	Medium	Medium
G3	High	High	High	High	High	High	Low	Low

4. Conclusions

Instead of extrusion or solvent casting method, the films are produced with the tape casting technique, which is environmentally friendly, provides wide size-length production opportunities and effective energy use. Depending on the nature of the selected raw materials and the amount of use, our inorganic powder (2.5% wt MicNo[®] ZnO) with a fixed morphology and amount gave different dispersion properties in polymer matrix composite material. This has caused us to obtain different results in the mechanical, optical, UV blocking, thermal, and % swelling properties of biodegradable composite films. When we look at the intersection of the features, it was seen that all the features we wanted were found in the films using low molecular weight chitosan with 15 (wt.%) PVA and 17 (v.%) glycerol.

The distribution of MicNo[®]-ZnO inorganic powder improved with increasing PVA-glycerol content and molecular weight of chitosan, which was supported by both XRD and SEM results. The increasing hydroxyl groups in the structure and the entanglement factor of the polymer chain accelerated the conversion of Zn²⁺ ions to ZnO. They supported the strong chemical interaction between the inorganic powder and the matrix. Homogeneous distribution of ZnO inorganic powders throughout the film as a result of increased intermolecular interactions resulted in an increase in the characteristic peak intensities of ZnO in XRD graphs and a smooth film surface by reducing the agglomerate tendency of ZnO inorganic powders in SEM analysis.

The prevention of agglomeration in the matrix and the improvement of the surface coverage property of ZnO were achieved by increasing the amount of PVA-glycerol, and the increase in the UV absorption capacity proved these results. With the increase in the molecular weight of chitosan, the UV absorbance values in the UVA-UVB regions decreased, but the transparency increased.

The increase in tensile strength and thermal stability is due to the intermolecular interaction between the inorganic powder and the polymeric structure. It was

supported by the results that the hydrogen bonds, crystallinity, and 3-D structure increased with the increase in the amount of PVA-glycerol and the molecular weight of chitosan, which improved mechanical and thermal stability.

Increasing the amount of PVA-glycerol and decreasing the molecular weight of chitosan caused a decrease in the amorphous structure, which reduced the % swelling capacity of the biodegradable films.

Achieving the desired properties for using biodegradable films in large-scale application fields, such as packaging material in the food industry and wound dressing in biomedical applications, depends on the effective utilization of the raw materials, creating a synergistic effect. The results we obtained in this study enabled us to develop a fundamental understanding of the relationship between the amounts of PVA and glycerol and the molecular weight of chitosan in the presence of new MicNo[®]-ZnO particles to create biodegradable films with specific application-dependent mechanical, thermal, optical and swelling properties. In addition, targets 12-14-15 of the Sustainable Development Goals adopted by the United Nations General Assembly can be made possible by biodegradable polymers that are friendly to waste management and greenhouse gas emissions, produced by understanding the synergistic effect of raw materials.

Disclosure statement

No potential conflict of interest was reported by the author(s).

Notes on contributors

Yeliz Köse is a research assistant at Bilecik Şeyh Edebali University. Topics of interest are nanomaterials, MicNo particles and biodegradable materials.

Ender Suvacı Founder & CTO at ENTEKNO Materials; Professor of Materials Science at Eskisehir Technical University. Topics of interest are particle synthesis, ceramic

processing, nanomaterials, MicNo particles and textured ceramics.

Acknowledgments

This research was supported financially by the Eskişehir Technical University Scientific Research Projects Commission (Project number: 20DRP036). The fruitful discussions provided by Prof. Dr. Murat Erdem and Mustafa Erdem Üreyen throughout this study are greatly acknowledged.

References

- [1] Stevens, E. S. Green Plastics: An Introduction to the New Science of Biodegradable Plastics. *J. Chem. Educ.* **2002**, *79*(9), 1031–1152. DOI: [10.1021/ed079p1072.1](https://doi.org/10.1021/ed079p1072.1).
- [2] Jayanth, D.; Kumar, P. S.; Nayak, G. C.; Kumar, J. S.; Pal, S. K.; Rajasekar, R. A Review on Biodegradable Polymeric Materials Striving Towards the Attainment of Green Environment. *J. Polym. Environ.* **2018**, *26*(2), 838–865. DOI: <https://doi.org/10.1007/s10924-017-0985-6>.
- [3] Biomaterials - Global Strategic Business Report. Global Industry Analysts. *Inc.* **2023**, ID, 5303108.
- [4] Anastas, P. T.; Zimmerman, J. B. Peer Reviewed: Design Through the 12 Principles of Green Engineering. *Environ. Sci. Technol.* **2003**, *37*(5), 94A–101A. DOI: [10.1021/es032373g](https://doi.org/10.1021/es032373g).
- [5] Mangiacapra, P.; Gorrasi, G.; Sorrentino, A.; Vittoria, V. Biodegradable Nanocomposites Obtained by Ball Milling of Pectin and Montmorillonites. *Carbohydr. Polym.* **2006**, *64*(4), 516–523. DOI: [10.1016/j.carbpol.2005.11.003](https://doi.org/10.1016/j.carbpol.2005.11.003).
- [6] Tsai, M. L.; Tseng, L. Z.; Chen, R. H. Two-Stage Microfluidization Combined with Ultrafiltration Treatment for Chitosan Mass Production and Molecular Weight Manipulation. *Carbohydr. Polym.* **2009**, *77*(4), 767–772. DOI: [10.1016/j.carbpol.2009.02.027](https://doi.org/10.1016/j.carbpol.2009.02.027).
- [7] Alishahi, A.; Aider, M. Applications of Chitosan in the Seafood Industry and Aquaculture: A Review. *Food Bioprocess Technol.* **2012**, *5*(3), 817–830. DOI: [10.1007/s11947-011-0664-x](https://doi.org/10.1007/s11947-011-0664-x).
- [8] Muzzarelli, R. A. A. Biomedical exploitation of chitin and chitosan via mechano-chemical disassembly, electrospinning, dissolution in imidazolium ionic liquids, and supercritical drying. *Mar. Drugs.* **2011**, *9*(9), 1510–1533. DOI: [10.3390/md9091510](https://doi.org/10.3390/md9091510).
- [9] Muzzarelli, R. A. A. Nanochitins and Nanochitosans, Paving the Way to Eco-Friendly and Energy-Saving Exploitation of Marine Resources. *Polym Sci: A Comp. R Reference.* **2012**, *10*, 153–164. DOI: [10.1016/B978-0-444-53349-4.00257-0](https://doi.org/10.1016/B978-0-444-53349-4.00257-0).
- [10] Jaworska, M.; Sakurai, K.; Gaudon, P.; Guibal, E. Influence of Chitosan Characteristics on Polymer Properties. I: Crystallographic Properties. *Polym. Int.* **2003**, *52*(2), 198–205. DOI: [10.1002/pi.1159](https://doi.org/10.1002/pi.1159).
- [11] Prasitsilp, M.; Jenwithisuk, R.; Kongsuwan, K. Cellular Responses to Chitosan in Vitro: The Importance of Deacetylation. *J. Mater. Sci. Mater. Med.* **2000**, *11*, 773–778. DOI: [10.1023/A:1008997311364](https://doi.org/10.1023/A:1008997311364).
- [12] Huang, M.; Khor, E.; Lim, L. Y. Uptake and Cytotoxicity of Chitosan Molecules and Nanoparticles: Effects of Molecular Weight and Degree of Deacetylation. *Pharmaceutical Research.* **2004**, *21*(2), 344–353. DOI: [10.1023/B:PHAM.0000016249.52831.a5](https://doi.org/10.1023/B:PHAM.0000016249.52831.a5).
- [13] Hsu, S.; Whu, S. W.; Tsai, C. L.; Wu, Y.-H.; Chen, H.-W.; Hsieh, K.-H. Chitosan as Scaffold Materials: Effects of Molecular Weight and Degree of Deacetylation. *J. Polym. Res.* **2004**, *11*(2), 141–147. DOI: [10.1023/B:JPOL.0000031080.70010.0b](https://doi.org/10.1023/B:JPOL.0000031080.70010.0b).
- [14] Kofuji, K.; Qian, C. J.; Nishimura, M.; Sugiyama, I.; Murata, Y.; Kawashima, S. Relationship Between Physicochemical Characteristics and Functional Properties of Chitosan. *Eur. Polym. J.* **2005**, *41*(11), 2784–2791. DOI: [10.1016/j.eurpolymj.2005.04.041](https://doi.org/10.1016/j.eurpolymj.2005.04.041).
- [15] Liu, Y.; Wang, S.; Zhang, R. Composite poly(lactic acid)/chitosan nanofibrous scaffolds for cardiac tissue engineering. *Int J Biol Macromol.* **2017**, *103*, 1130–1137. DOI: [10.1016/j.ijbiomac.2017.05.101](https://doi.org/10.1016/j.ijbiomac.2017.05.101).
- [16] Wang, H.; Zhang, R.; Zhang, H.; Jiang, S.; Liu, H.; Sun, M.; Jiang, S. Kinetics and Functional Effectiveness of Nisin Loaded Antimicrobial Packaging Film Based on Chitosan/Poly (Vinyl Alcohol). *Carbohydr. Polym.* **2015**, *127*, 64–71. DOI: [10.1016/j.carbpol.2015.03.058](https://doi.org/10.1016/j.carbpol.2015.03.058).
- [17] Pathan, S. G.; Fitzgerald, L. M.; Ali, S. M.; Damrauer, S. M.; Bide, M. J.; Nelson, D. W.; Ferran, C.; Phaneuf, T. M.; Phaneuf, M. D. Cytotoxicity Associated with Electrospun Polyvinyl Alcohol. *J. Biomed. Mater. Res. Part B.* **2015**, *103*(8), 1652–1662. DOI: [10.1002/jbm.b.33337](https://doi.org/10.1002/jbm.b.33337).
- [18] Halima, N. B. Poly(vinyl Alcohol): Review of Its Promising Applications and Insights into Biodegradation. *R.S.C. Adv.* **2016**, *6*(46), 39823–39832. DOI: [10.1039/C6RA05742J](https://doi.org/10.1039/C6RA05742J).
- [19] Kochkina, N. E.; Lukin, N. D. Structure and Properties of Biodegradable Maize Starch/Chitosan Composite Films as Affected by PVA Additions. *Int J Biol Macromol.* **2020**, *157*, 377–384. DOI: [10.1016/j.ijbio mac.2020.04.154](https://doi.org/10.1016/j.ijbio mac.2020.04.154).
- [20] Sofla, M. S. K.; Mortazavi, S.; Seyfi, J. Preparation and Characterization of Polyvinyl Alcohol/Chitosan Blends Plasticized and Compatibilized by Glycerol/Polyethylene Glycol. *Carbohydr. Polym.* **2020**, *232*, 115784. DOI: [10.1016/j.carbpol.2019.115784](https://doi.org/10.1016/j.carbpol.2019.115784).
- [21] Yin, M.; Lin, X.; Ren, T.; Li, Z.; Ren, X.; Huang, T. S. Cytocompatible Quaternized Carboxymethyl Chitosan/Poly(vinyl Alcohol) Blend Film Loaded Copper for Antibacterial Application. *Int J Biol Macromol* **2018**, *120*, 992–998. Part A. DOI: [10.1016/j.ijbiomac.2018.08.105](https://doi.org/10.1016/j.ijbiomac.2018.08.105).
- [22] Liu, Y.; Wang, S.; Lan, W. Fabrication of Antibacterial Chitosan-PVA Blended Film Using Electro spray Technique for Food Packaging Applications. *Int J Biol Macromol* **2018**, *107*, 848–854. Part A. DOI: [10.1016/j.ijbiomac.2017.09.044](https://doi.org/10.1016/j.ijbiomac.2017.09.044).
- [23] Kim, S.; Lim, H.; Kim, S.; Lee, D. Y. Effect of PVA Concentration on Strength and Cell Growth Behavior of PVA/Gelatin Hydrogels for Wound Dressing. *J. Biomed. Eng. Res.* **2020**, *41*, 1–7. DOI: [10.9718/JBER.2020.41.1.1](https://doi.org/10.9718/JBER.2020.41.1.1).

- [24] Huie, J.; Suqiu, Z.; Haiyan, J.; Zhijian, L.; Lijuan, C.; Nihao, L.; Xinhua, L. Microporous Chitosan/Polyvinyl Alcohol Based Active Packaging Materials with Integrated Gas-Transmission, Radiation-Cooling, Anti-Microbial, and Ultraviolet Shielding Features. *Chem. Eng. J.* **2023**, *473*, 145432. DOI: [10.1016/j.cej.2023.145432](https://doi.org/10.1016/j.cej.2023.145432).
- [25] Priyadarshi, R.; Sauraj, K. B.; Negi, Y. S. Chitosan Films Incorporated with Citric Acid and Glycerol as an Active Packaging Material for Extension of Green Chilli Shelf Life. *Carbohydr. Polym.* **2018**, *195*, 329–338. DOI: [10.1016/j.carbpol.2018.04.089](https://doi.org/10.1016/j.carbpol.2018.04.089).
- [26] Cazón, P.; Velázquez, G.; Vázquez, M. Bacterial Cellulose Films: Evaluation of the Water Interaction. *Food Packag. Shelf Life.* **2020**, *25*, 100526. DOI: [10.1016/j.fpsl.2020.100526](https://doi.org/10.1016/j.fpsl.2020.100526).
- [27] Vázquez, M.; Velázquez, G.; Cazón, P. UV-Shielding Films of Bacterial Cellulose with Glycerol and Chitosan. Part 1: Equilibrium Moisture Content and Mechanical Properties. *CyTA - J. Food.* **2021**, *19*(1), 105–114. DOI: [10.1080/19476337.2020.1870566](https://doi.org/10.1080/19476337.2020.1870566).
- [28] Cazón, P.; Vázquez, M.; Velázquez, G. Composite Films with UV-Barrier Properties of Bacterial Cellulose with Glycerol and Poly (Vinyl Alcohol): Puncture Properties, Solubility, and Swelling Degree. *Biomacromolecules.* **2019**, *20*(5), 2084–2095. DOI: [10.1021/acs.biomac.9b00317](https://doi.org/10.1021/acs.biomac.9b00317).
- [29] Vázquez, M.; Velázquez, G.; Cazón, P. UV-Shielding Films of Bacterial Cellulose with Glycerol and Chitosan. Part 2: Structure, Water Vapor Permeability, Spectral and Thermal Properties. *CyTA - J. Food.* **2021**, *19*(1), 115–126. DOI: [10.1080/19476337.2020.1870565](https://doi.org/10.1080/19476337.2020.1870565).
- [30] Peponi, L.; Puglia, D.; Torre, L.; Valentini, L.; Kenny, J. M. Processing of Nanostructured Polymers and Advanced Polymeric Based Nanocomposites. *Mater. Sci. Eng. R.* **2014**, *85*, 1–46. DOI: [10.1016/j.mser.2014.08.002](https://doi.org/10.1016/j.mser.2014.08.002).
- [31] Köse, Y.; Suvacı, E.; Atlı, B. Improving Properties of Biodegradable Chitosan/PVA Composite Polymers via Novel Designed ZnO Particles. *J. Aust. Ceram. Soc.* **2023**, *59*(1), 245–257. DOI: [10.1007/s41779-022-00830-2](https://doi.org/10.1007/s41779-022-00830-2).
- [32] Hezma, A. M.; Rajeh, A.; Mannaa, M. A. An Insight into the Effect of Zinc Oxide Nanoparticles on the Structural, Thermal, Mechanical Properties and Antimicrobial Activity of Cs/PVA Composite. *Colloids Surf. A.* **2019**, *581*(20), 123821. DOI: [10.1016/j.colsurfa.2019.123821](https://doi.org/10.1016/j.colsurfa.2019.123821).
- [33] Hemalatha, K. S.; Rukmani, K.; Suriyamurthy, N.; Nagabhushana, B. M. Synthesis, Characterization and Optical Properties of Hybrid PVA-Zno Nanocomposite: A Composition Dependent Study. *Mater. Res. Bull.* **2014**, *51*, 438–446. DOI: [10.1016/j.materresbull.2013.12.055](https://doi.org/10.1016/j.materresbull.2013.12.055).
- [34] Azizi, S.; Ahmad, M. B.; Ibrahim, N. A.; Hussein, M. Z.; Namvar, F. Cellulose Nanocrystals/Zno as a Bifunctional Reinforcing Nanocomposite for Poly(vinyl Alcohol)/Chitosan Blend Films: Fabrication, Characterization and Properties. *Int. J. Mol. Sci.* **2014**, *15*(6), 11040–11053. DOI: [10.3390/ijms150611040](https://doi.org/10.3390/ijms150611040).
- [35] Chen, R. H.; Hwa, H.-D. Effect of Molecular Weight of Chitosan with the Same Degree of Deacetylation on the Thermal, Mechanical, and Permeability Properties of the Prepared Membrane. *Carbohydr. Polym.* **1996**, *29*(4), 353–358. DOI: [10.1016/S0144-8617\(96\)00007-0](https://doi.org/10.1016/S0144-8617(96)00007-0).
- [36] Bajpai, S. K.; Chand, N.; Chaurasia, V. Investigation of Water Vapor Permeability and Antimicrobial Property of Zinc Oxide Nanoparticles-Loaded Chitosan-Based Edible Film. *J. Appl. Polym. Sci.* **2010**, *115*(2), 674–683. DOI: [10.1002/app.30550](https://doi.org/10.1002/app.30550).
- [37] Dionisio, M.; Ricci, L.; Pecchini, G.; Masseroni, D.; Ruggeri, G.; Cristofolini, L.; Rampazzo, E.; Dalcanale, E. Polymer Blending Through Host-Guest Interactions. *Macromolecules.* **2014**, *47*(2), 632–638. DOI: [10.1021/ma401506t](https://doi.org/10.1021/ma401506t).
- [38] Rashmi, S. H.; Raizada, A.; Madhu, G. M.; Kittur, A. A.; Suresh, R.; Sudhina, H. K. Influence of Zinc Oxide Nanoparticles on Structural and Electrical Properties of Polyvinyl Alcohol Films. *Plast. Rubber Compos.* **2015**, *44*(1), 33–39. DOI: [10.1179/1743289814Y.0000000115](https://doi.org/10.1179/1743289814Y.0000000115).
- [39] Su, L.; Huang, J.; Li, H.; Pan, Y.; Zhu, B.; Zhao, Y.; Liu, H. Chitosan-Riboflavin Composite Film Based on Photodynamic Inactivation Technology for Antibacterial Food Packaging. *Int J Biol Macromol.* **2021**, *172*, 231–240. DOI: [10.1016/j.ijbiomac.2021.01.056](https://doi.org/10.1016/j.ijbiomac.2021.01.056).
- [40] El-Ahdal, M. A. Radiation Effect on the Molecular Structure of Dyed Poly(vinyl Alcohol). *Int. J. Polym. Mater.* **2001**, *48*(1), 17–28. DOI: [10.1080/00914030008048376](https://doi.org/10.1080/00914030008048376).
- [41] Liu, D.; Wei, Y.; Yao, P.; Jiang, L. Determination of the Degree of Acetylation of Chitosan by UV Spectrophotometry Using Dual Standards. *Carbohydr. Res.* **2006**, *341*(6), 782–785. DOI: [10.1016/j.carres.2006.01.008](https://doi.org/10.1016/j.carres.2006.01.008).
- [42] Abdeen, Z. Swelling and Swelling Characteristics of Cross-Linked Poly(vinyl Alcohol)/Chitosan Hydrogel Film. *J Dispers. Sci. Technol.* **2011**, *32*(9), 1337–1344. DOI: [10.1080/01932691.2010.505869](https://doi.org/10.1080/01932691.2010.505869).
- [43] Wang, Q.; Du, Y. M.; Fan, L. H. Properties of Chitosan/Poly(vinyl Alcohol) Films for Drug Controlled Release. *J. Appl. Polym. Sci.* **2005**, *96*(3), 808–813. DOI: [10.1002/app.21518](https://doi.org/10.1002/app.21518).
- [44] Pelissari, F. M.; Yamashita, F.; Grossmann, M. V. E. Extrusion Parameters Related to Starch/Chitosan Active Films Properties. *Int. J. Food Sci. Technol.* **2011**, *46*(4), 702–710. DOI: [10.1111/j.1365-2621.2010.02533.x](https://doi.org/10.1111/j.1365-2621.2010.02533.x).
- [45] Ma, J.; Xin, C.; Tan, C. Preparation, Physicochemical and Pharmaceutical Characterization of Chitosan from *Catharsius Molossus* Residue. *Int J Biol Macromol.* **2015**, *80*, 547–556. DOI: [10.1016/j.ijbiomac.2015.07.027](https://doi.org/10.1016/j.ijbiomac.2015.07.027).
- [46] Stachowiak, N.; Kowalonek, J.; Kozłowska, J. Effect of Plasticizer and Surfactant on the Properties of Poly (vinyl Alcohol)/Chitosan Films. *Int J Biol Macromol.* **2020**, *164*(1), 2100–2107. DOI: [10.1016/j.ijbiomac.2020.08.001](https://doi.org/10.1016/j.ijbiomac.2020.08.001).
- [47] Mishra, S. K.; Kannan, S. Development, Mechanical Evaluation and Surface Characteristics of Chitosan/

- Polyvinyl Alcohol Based Polymer Composite Coatings on Titanium Metal. *J. Mech. Behav. Biomed. Mater.* **2014**, *40*, 314–324. DOI: [10.1016/j.jmbbm.2014.08.014](https://doi.org/10.1016/j.jmbbm.2014.08.014).
- [48] Peng, Z.; Kong, L. X. A Thermal Degradation Mechanism of Polyvinyl Alcohol/Silica Nanocomposites. *Polym. Degrad. Stab.* **2007**, *92*(6), 1061–1071. DOI: [10.1016/j.polydegradstab.2007.02.012](https://doi.org/10.1016/j.polydegradstab.2007.02.012).
- [49] Chandrakala, H. N.; Ramaraj, B.; Shivakumaraiah, S. Optical properties and structural characteristics of zinc oxide a cerium oxide doped polyvinyl alcohol films. *J. Alloys Compd.* **2014**, *586*, 333–342. DOI: [10.1016/j.jallcom.2013.09.194](https://doi.org/10.1016/j.jallcom.2013.09.194).
- [50] Wanjun, T.; Cunxin, W.; Donghua, C. Kinetic Studies on the Pyrolysis of Chitin and Chitosan. *Polym. Degrad. Stab.* **2005**, *87*(3), 389–394. DOI: [10.1016/j.polydegradstab.2004.08.006](https://doi.org/10.1016/j.polydegradstab.2004.08.006).
- [51] Abdeen, Z. I.; El Farargy, A. F.; Negm, N. A. Nanocomposite Framework of Chitosan/Polyvinyl Alcohol/ZnO: Preparation, Characterization, Swelling and Antimicrobial Evaluation. *J. Mol. Liq.* **2018**, *250*, 335–343. DOI: [10.1016/j.molliq.2017.12.032](https://doi.org/10.1016/j.molliq.2017.12.032).
- [52] Kim, S. J.; Lee, K. J.; Kim, I. Y.; Kim, S. I. Swelling Kinetics of Interpenetrating Polymer Hydrogels Composed of Poly(vinyl Alcohol)/Chitosan. *J. Macromol. Sci. A.* **2003**, *40*(5), 501–510. DOI: [10.1081/MA-120019888](https://doi.org/10.1081/MA-120019888).
- [53] Sung, J. H.; Hwang, M. R.; Kim, J. O.; Lee, J. H.; Kim, Y. I.; Kim, J. H.; Chang, S. W.; Jin, S. G.; Kim, J. A.; Lyoo, W. S., et al. Gel Characterization and in vivo Evaluation of Minocycline-Loaded Wound Dressing with Enhanced Wound Healing Using Poly(vinyl Alcohol) and Chitosan. *Int. J. Pharm.* **2010**, *392*(1–2), 232–240. DOI: [10.1016/j.ijpharm.2010.03.024](https://doi.org/10.1016/j.ijpharm.2010.03.024).
- [54] Chien, R. C.; Yen, M. T.; Mau, J. L. Antimicrobial and Antitumor Activities of Chitosan from Shiitake Stipes, Compared to Commercial Chitosan from Crab Shell. *Carbohydr. Polym.* **2016**, *138*, 259–264. DOI: [10.1016/j.carbpol.2015.11.061](https://doi.org/10.1016/j.carbpol.2015.11.061).
- [55] Bano, I.; Arshad, M.; Yasin, T.; Ghauri, M. A. Preparation, Characterization and Evaluation of Glycerol Plasticized Chitosan/PVA Blends for Burn Wounds. *Int J Biol Macromol.* **2019**, *124*, 155–162. DOI: [10.1016/j.ijbiomac.2018.11.073](https://doi.org/10.1016/j.ijbiomac.2018.11.073).
- [56] Yan, J.; Li, M.; Wang, H.; Lian, X.; Fan, Y.; Xie, Z.; Niu, B.; Li, W. Preparation and Property Studies of Chitosan-PVA Biodegradable Antibacterial Multilayer Films Doped with Cu₂O and Nano-Chitosan Composites. *Food Control.* **2021**, *126*, 108049. DOI: [10.1016/j.foodcont.2021.108049](https://doi.org/10.1016/j.foodcont.2021.108049).